John Wuest
Dr., Civil Engineer
Ecole Polytechnique Fédérale de Lausanne
Lausanne, Switzerland

Emmanuel Denarié
Senior Scientist, Dr., Civil Engineer
Ecole Polytechnique Fédérale de Lausanne
Lausanne, Switzerland

Eugen Brühwiler
Prof., Dr., Civil Engineer
Ecole Polytechnique Fédérale de Lausanne
Lausanne, Switzerland

Model for predicting the UHPFRC tensile hardening response

Summary

Ultra High Performances Fibre Reinforced Concretes (UHPFRC) are characterised by an extremely low permeability and outstanding mechanical properties. These characteristics make UHPFRC suitable for locally "harden" reinforced concrete structures subjected to aggressive environments and/or mechanical stresses. Results from uni-axial tensile tests on different UHPFRC materials and cast in different directions have shown a variety of mechanical behaviour. In particular, the hardening behaviour ranges from 0.1-0.4 % but is, in some cases, not existent. A meso-mechanical model is developed to predict the UHPFRC tensile response as a function of the volume, aspect-ratio, distribution and orientation of the fibres and the mechanical properties of the matrix. The model allows determining the effect of two parameters, the coefficient of orientation and the volume of fibre, on the hardening behaviour.

Keywords: *UHPFRC, strain hardening, fibre orientation, simulation model.*

1 Introduction

More and more durability and load carrying capacity problems emerge from aging existing civil structures. In order to solve these problems, UHPFRC materials are being employed because of their easy on-site casting combined with their excellent strength and durability properties. The tensile performances of these materials are dependent on various factors such as the quality of the matrix, the orientation and distribution of the fibres, the aspect-ratio and the volume of fibres.

In [1], the fibre orientation and distribution in two specimens constituted from different fibrous mixes, which showed dissimilar hardening behaviour, were investigated through image analysis. Unfortunately, even if a difference was observed, it was not directly possible to determine if the fibre orientation was responsible of the increase of the hardening domain. Moreover, [1] tested also two specimens (same mix) cast in different directions. The results showed two very dissimilar behaviours in tension (hardening-softening and only softening). In this case the fibre orientation analysis showed a significant difference in the coefficient of orientation which explained the different tensile responses observed. Moreover, the different models developed by [2], [3], [4],

[5] to determine the response of fibre reinforced composite are not sufficient for predicting the extent of the hardening domain in UHPFRC.
These two remarks emphasize the need of the development of a novel meso-mechanical model that allows predicting the hardening domain in tension based on the factors mentioned above.

2 Materials and experimental results

2.1 Materials properties

The tensile behaviour of three materials is studied in this paper. The first two UHPFRC (UHPFRC-1 and 2) investigated contain a high amount of cement (>1000 kg/m^3), a relatively high quantity of steel fibres (4-6%) and has a low water/cement ratio (<0.15). A higher aspect ratio of the fibres was used for UHPFRC 2 compared to UHPFRC 1 leading to a decrease in fibre volume in order to obtain sufficient workability. The third material is an ECC developed and tested by [6] and had 2% by volume of PVA fibres.

2.2 Experimental results

UHPFRC-1 and 2 were tested using dogbone specimens with a total length of 700 mm, with a constant cross-section of 5000 mm^2 (100x50 mm) over a length of 300 mm. The measurements were done over a 350 mm distance (figure 2). The ECC was also studied with a dogbone specimen with a constant cross-section of 968 mm^2 over a length of 185 mm. All specimens were cast horizontally.
UHPFRC-2 and ECC had a significant hardening domain, i. e. 0.24% and 1% respectively. Contrary to this, UHPFRC-1 had a more limited hardening domain (0.1%). The fibre orientation and distribution were investigated in [1] on one specimen of each UHPFRC group (Table 1). The results show that the UHPFRC-2 has highly oriented fibres parallel to the principle stress compared to UHPFRC-1, which helps increasing the hardening domain.

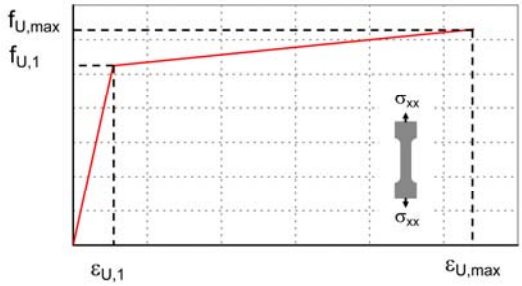

Figure 1: Description of the parameters of a tensile test response mentionned in table 1

Table 1: Tensile test results for the three groups of tested specimens

		Group specimen results				Selected specimen results			
		$\varepsilon_{U,1}$ [%]	$f_{U,1}$ [MPa]	$\varepsilon_{U,max}$ [%]	$f_{U,max}$ [MPa]	$\varepsilon_{U,1}$ [%]	$f_{U,1}$ [MPa]	$\varepsilon_{U,max}$ [%]	$f_{U,max}$ [MPa]
UHPFRC-1	Average	0.018	9.0	0.07	9.65	0.021	10	0.1	10.7
	Std. Dev.	0.002	0.9	0.02	0.7				
UHPFRC-2	Average	0.027	10.5	0.27	12.6	0.032	11.5	0.24	13
	Std. Dev.	0.006	1.0	0.06	1.4				
ECC	Average	-	3.11	0.99	4.89	Not mentionned			
	Std. Dev.		0.23	0.57	0.07				

3 Mechanical model of random micro cracking

The model for predicting the response in tension of hardening-softening cementitious materials is explained in details in [7] and consists of two parts:

- Sectional model of one micro-crack

This part of the model was adapted from the approach developed by [9]. It consists in the superposition of the matrix softening behaviour (σ_m), the pre-stress already present in the fibre before cracking (σ_{fps}) and the fibre bridging (σ_{fb}) to predict the sectional response.

$$\sigma_U(w) = \sigma_{fps}(w) + \sigma_{fb}(w) + \sigma_m(w) \quad (1)$$

The fibre bridging is considered by equation 2 which corresponds to the summation of the contribution of all the fibres depending of their out of plane angle f(θ).

$$F_{fb} = \sum_{i=0}^{n_f} F_{fb,i} \cdot f(\theta) \quad (2)$$

The force bridged by each fibre ($F_{fb,i}$) for a crack opening (w) can be calculated using equations 3 and 4 depending on the crack opening.

$$F_{fb,i} = \sqrt{\frac{\pi^2 \tau_0 E_f {d_f}^3 (1+\eta)}{4} w} \qquad 0 < w < w_{db} \quad (3)$$

$$F_{fb,i} = \pi d_f \tau (L_e - w + w_{db}) \qquad w_{db} < w < w_{db} + L_e \quad (4)$$

$$w_{db} = \frac{4\tau_0 {L_e}^2}{E_f d_f (1+\eta)} \qquad \eta = V_f E_f / (V_m E_m) \quad (5)$$

$$\tau = \tau_0((L_e + w_{db}) - w_{db})w + \tau_0(1 + \frac{w_{db}}{(L_e + w_{db} - w_{db})}) \quad (6)$$

With w_{db}: crack opening at which full debonding is complete; d_f : fibre diameter; V_f: fibre volume; V_m: Matrix volume; E_f: Fibre module of elasticity; E_m: Matrix module of elasticity.

The hypotheses considered are a constant frictional stress τ_0 during the debonding process, a uniform distribution of the fibre embedment length (L_e) and the decay of the frictional stress with increasing crack opening (equation 6).

- Combination of discretely distributed micro-cracks

Potential cracks spaced every 0.02 mm are created on all the tensile specimen length. They are activated if the stress exceeds the first cracking resistance ($f_{U,1}$). The first cracking resistance is randomly distributed over the specimen length following a normal distribution. The average and standard-deviation are deduced from the experimental results.
The stress releases in the neighbourhood of propagating micro-cracks locally prevent creating a further micro-crack. Moreover, in the model, the stress increases until one of the sections can no more withstand it and enters into the softening behaviour.
The total displacement is calculated using equation 7 which takes into account the elastic displacement of the un-cracked part and the contribution of all the opening cracks. A similar approach has been suggested in [10].

$$\Delta l = \sum_{i=0}^{N} w_i(\sigma_u) + \frac{\sigma_u}{E_u} L_R \qquad (7)$$

The hypothesis considered in this part of the model is that only the resistance of the matrix varies.

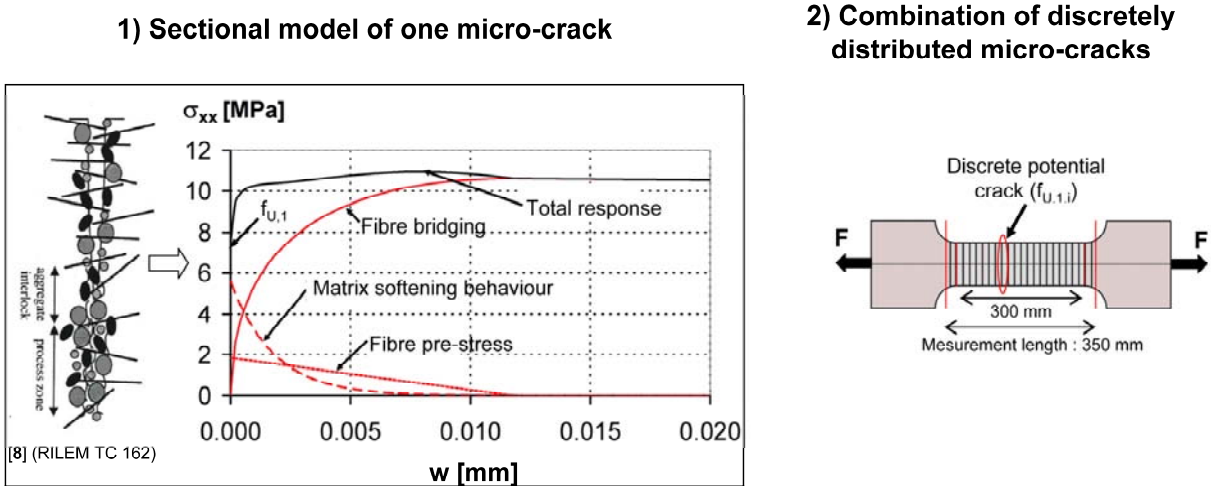

Figure 2: Description of the two parts of the model

4 Validation

The model is validated using the results of the three tensile tests described in section 2.2.
The parameters used in the simulation are given in table 2. For UHPFRC-1 all the properties are directly obtained from the experimental results.

Table 2: Description of the parameter used in the simulation (G_F is the matrix fracture energy, $F_{f,R}$ is the fibre maximum resistance in tension and G_d is the chemical bond between the fibre and the matrix)

		UHPFRC-1	UHPFRC-2	ECC
Sectional model of a micro-crack	τ_0 [MPa]	6.9	6.5	2.44
	G_d [J/m^2]	-	-	4.71
	C_{OR} [-]	0.24	0.66	0.43
	V_f [%]	6.39	4.27	2.00
	E_f [MPa]	210'000	210'000	48'000
	E_m [MPa]	40'000	40'000	15'900
	L_f [mm]	10	13	12
	d_f [mm]	0.2	0.16	0.039
	G_F [J/m^2]	10	10	50
	$F_{f,R}$ [MPa]	3200	2500	1000
Combination of discretly distributed micocracks	E_U [J/m^2]	49'000	52'000	16'438
	$f_{U,1,sim}$ (Average) [MPa]	10.1	13.5	4.6
	$f_{U,1,sim}$ (Std. Dev.) [MPa]	0.7	1.2	0.6

For UHPFRC-2, the frictional stress (τ_0) is obtained by back analysis of the ultimate resistance of the specimen ([7]). For the ECC, the parameters were found in [6] and [11]. Only the coefficient of orientation is determined by back analysis of the ultimate tensile resistance.

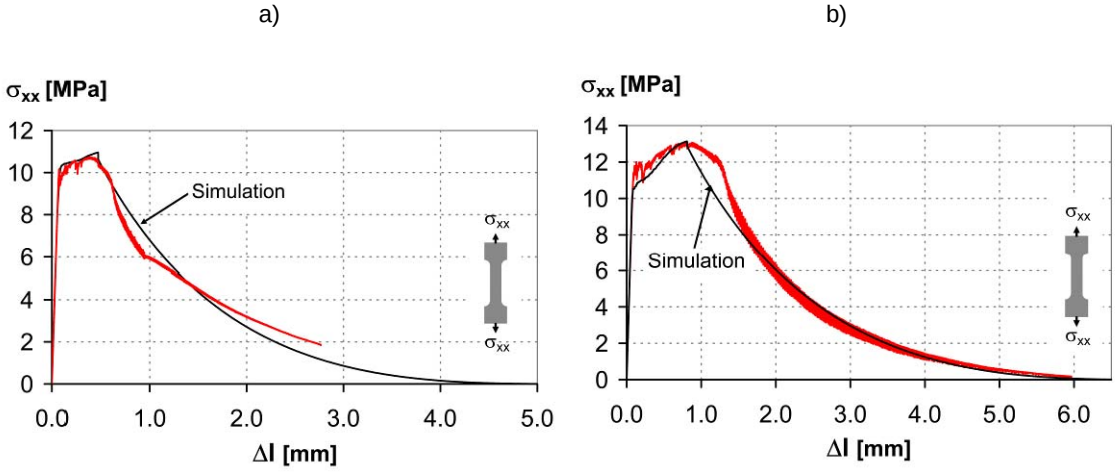

Figure 3: Comparing experimental and simulation results: a) UHPFRC-1; b) UHPFRC-2

For the two UHPFRC materials tested, a good correspondence between the simulations and the tensile test response is obtained in terms of the shape of the curves and the extent of the hardening domain. The model does however not perfectly follow the experimentally measured softening curves; this is due to the configuration of the test used. Dogbone specimens, which are

less adapted for measuring the softening domain ([7]), were employed and explain the obtained difference in shape.

The last validation is done using the ECC. In this situation, the equation for the fibre pull-out has to be modified to take into account the chemical bond (G_d).

$$P = \sqrt{\frac{\pi^2 \tau_0 E_f {d_f}^3 (1+\eta)}{4} w + \frac{\pi^2 G_d E_f {d_f}^3}{2}} \qquad (8)$$

We can observe on figure 4 that the model is able to reproduce the extent, the shape of the hardening domain and the drop after the peak resistance due to fibre rupture.

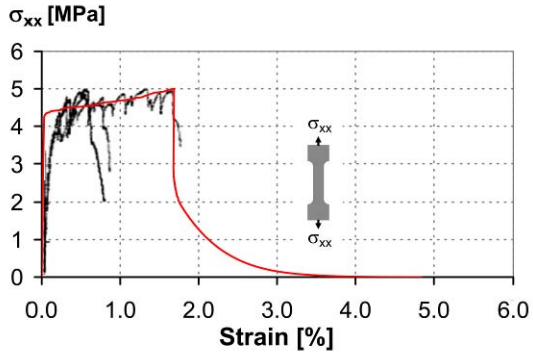

Figure 4: Comparing experimental and simulation results for the ECC

On the other side, the model gives a more rigid response in the elastic domain than the experimentally measured one; this is mostly due to the lack of information on this material, particularly the modulus of elasticity.

5 Parametric study

Two parameters will be investigated in this study: the effect of the coefficient of orientation and the fibre volume.

a) Coefficient of orientation

The effect of the coefficient of orientation is investigated using the same parameters as in table 1 for the specimens UHPFRC-1 and 2 but varying the coefficient of orientation from 0.56 to 1.

As can be seen on figure 5 a), the use of a coefficient of orientation of 0.56 for mix 2, leads to a response which is similar to the smallest tensile test of the group. Thus, all the tested specimens should present a coefficient of orientation higher than 0.56 if we consider the hypothesis of a constant volume of fibre. Moreover, the development of cracks is increased with the use of a higher coefficient of orientation, leading to an extended hardening domain. As can be seen on figure 5 b), the mix 2, which has fibres with a higher aspect ratio has always an increased hardening domain compared to mix 1 for the same coefficient of orientation. This is mainly due to the fact that the fibre of mix 2 requires a higher force before being pulled-out.

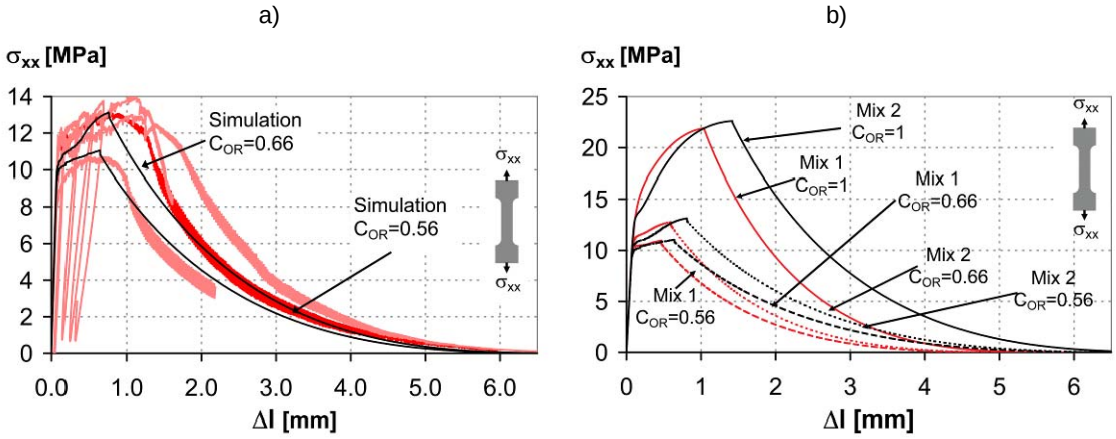

Figure 5: a) Comparison between the simulation with a C_{OR} of 0.56 and the experimental resullts for UHPFRC-2; b) Effect of the C_{OR} on the tensile response for Mix 1 and 2

Also, these fibres are more effective at bridging a crack. In other words, they allow withstanding a larger crack opening with the same force compared to those used in mix 1.

b) Volume of fibre

The effect of the volume of fibre is investigated on the two same mixes than in the previous study. The volume of fibre is varied between 5 and 9 % and between 3 and 6 % for Mix 1 and Mix 2 respectively.

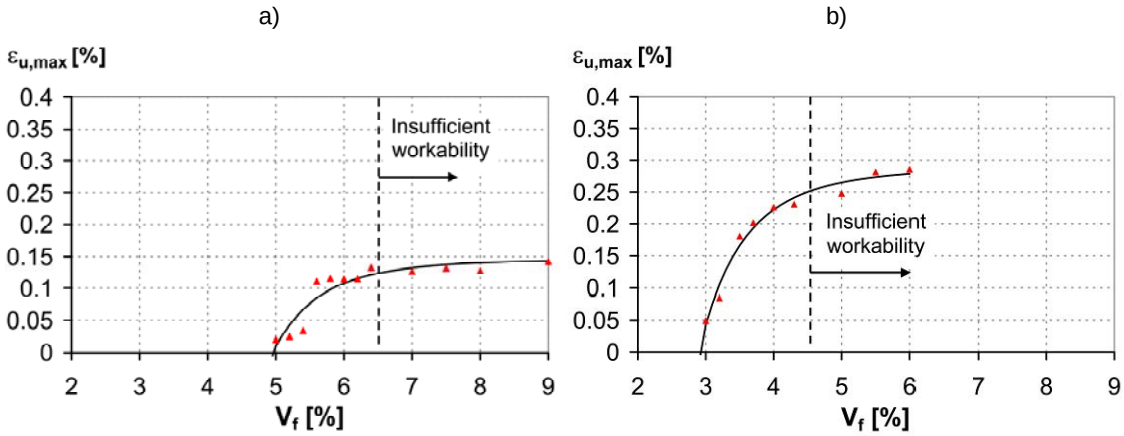

Figure 6: Extent of the hardening domain as a function of Volume of fibre: a) Mix 1; b) Mix 2

The extent of the hardening domain does not increase linearly with increasing volume of fibre but tends to an asymptotic value (figure 6); i. e. with Mixes 1 and 2 a maximum hardening domain of about 0.15 and 0.3 % respectively may be reached. It is important to point out that the slope of the hardening domain versus volume of fibre is more important for mix 2. A decrease of the fibre volume has thus a more significant effect on the hardening behaviour for mix 2. Moreover, mix 1 seems to be more effective with respect to the use of the hardening domain. Assuming that the mix is still applicable with high volume of fibre, Mix 1 (V_f=6%) has already attained

it's asymptotic value while in mix 2 (V_f=4%) it is still necessary to increase the volume of fibre before attaining the asymptotic value.

6 Conclusions

- A novel meso-mechanical model was developed and validated with experimental results in order to predict the extent of the hardening domain for different cementitious materials.
- The orientation of the fibres in the specimen has a significant impact on the hardening response. A coefficient of orientation smaller than 0.64 does not allow creating an extended hardening behaviour.
- The tensile hardening response of mixes with a high fibre aspect-ratio and lower dosages are more sensitive to a variation of the fibre dosage.

7 Acknowledgments

The Swiss State Secretariat for Education and Research (SER) in the context of the European project Suinstainable and Advanced Materials for Roads Infrastructures (SAMARIS) have financially supported this research.

8 References

[1] Wuest J., Denarié E., Brühwiler E.: Measurement and modelling of fibre distribution and orientation in UHPFRC. In: Proc. HPFRCC5, Proceedings PRO 53, Mainz, pp. 259-266, 2007.

[2] Naaman A.: Strain hardening and deflection hardening fiber reinforced cement composites. In: Proc. HPFRCC4, Proceedings Pro 30, Ann Arbor, pp.95-113.

[3] Li V. C., Leung C. K. Y.: Steady-State and Multiple Cracking of Short Random Fiber Composites. In: ASCE Journal of Engineering Mechanics 188, No 11, pp. 2246-2264, 1992.

[4] Pfyl T.: Tragverhalten von Stahlfaserbeton. PhD Thesis ETH, N°15005, Zürich, 2003. (in German).

[5] Markovic I.: High-Performance hybrid-Fibre Concrete : Developpement and Utilisation. PhD Thesis, TU Delft, Delft, 2006.

[6] Li V. C., Wu C., Wang S., Ogawa A., Saito T.: Interface tailoring for Strain-hardening Polyvinyl Alcohol- Engineered Cementitious Composites (PVA-ECC). In: ACI Materials Journal 99, No 5, pp. 463-472, 2002.

[7] Wuest J.: Comportement structural des Bétons de Fibres Ultra Performants en traction dans des éléments composes. PhD Thesis, N° 3987, EPFL, Lausanne, 2007. (In French, submitted).

[8] RILEM TC 162-TDF: Test and Design Methods for Steel Fibre Reinforced Concrete. In: Materials and Structures 35, pp.579-582, 2002.

[9] Li V. C., Stang H., Krenchel H.: Micromechanics of crack bridging in fibre-reinforced concrete. In: Materials and Structures 26, pp.486-494, 1993.

[10] Yang J., Fischer G.: Simulation of the tensile stress-strain behaviour of strain hardening cementitious composites. In: Proc. Measuring, Monitoring and Modelling Concrete Properties, Alexandroupolis, pp. 25-31, 2006.

[11] Kanda T., LI V. C.: Practical Design Criteria for Satured Pseudo Strain Hardening Behavior in ECC. In: Journal of Advanced Concrete Technology 4, No 1, pp. 59-72, 2006.